

UNCLASSIFIED

Defense Technical Information Center  
Compilation Part Notice

ADP010823

TITLE: High Resolution Imaging from the  
Geostationary Orbit

DISTRIBUTION: Approved for public release, distribution unlimited  
Availability: Document partially illegible.

This paper is part of the following report:

TITLE: Space-Based Observation Technology

To order the complete compilation report, use: ADA391327

The component part is provided here to allow users access to individually authored sections of proceedings, annals, symposia, ect. However, the component should be considered within the context of the overall compilation report and not as a stand-alone technical report.

The following component part numbers comprise the compilation report:

ADP010816 thru ADP010842

UNCLASSIFIED

# High Resolution Imaging from the Geostationary Orbit

Massimo Cecconi (\*), Stefano Cesare (\*), Cesare Dionisio (\*\*)

(\*) ALENIA AEROSPAZIO, Divisione Spazio, C.so Marche 41, 10146 Torino, Italia  
Fax 011-7180998, [scesare@to.alespazio.it](mailto:scesare@to.alespazio.it), [mceccconi@to.alespazio.it](mailto:mceccconi@to.alespazio.it)

(\*\*) ALENIA AEROSPAZIO, Divisione Spazio, V. Saccomuro 24, 00131, Roma, Italia  
Fax 06-4191391, [c.dionisio@rmmail.alespazio.it](mailto:c.dionisio@rmmail.alespazio.it),

## Introduction

The geostationary orbit (GEO) is commonly used for telecommunication and meteorological missions, rarely for scientific missions, within certain limit for remote sensing. For this purpose, low orbits (LEO), typically between 500 to 1,000 km in altitude, are employed in order to get higher spatial and radiometric resolutions. However the GEO offers several advantages for the earth observations, which are: possibility of a continuous observations of the same geographic area of interest, coverage of the whole hemisphere and possibility of re-visiting in a short time the same region, real-time dissemination of the data towards the users and constant observation angles. These features are particularly important in the tactical and strategic surveillance.

The distance from the Earth (about 36,000 km) represents the main obstacle to the full exploitation of the GEO orbit for the remote sensing. This implies that, to achieve a given spatial resolution and to collect a given photon flux at a given observation wavelength, an instrument with aperture tens of times larger than those employed in LEO must be utilized in GEO. For example, to perform ground observation at very high spatial resolution of about 1 meter in the visible spectral band with a monolithic-mirror telescope, an aperture of about 30-m would be required.

With a monolithic-mirror telescope the resolution increase associated to a large aperture is paid first of all in terms of instrument mass. A large primary mirror implies, in addition, the need of the availability of a large volume under the launcher fairing for the accommodation of the instrument.

A solution to the problems related to the large aperture, in the cases when the issue is the high resolution and not the light collection (like for the observation of a portion of the Earth surface), is represented by the synthetic aperture technique. It consists in the reconstruction of the original image of an object starting from that formed on the common focal plane of a set of telescopes (or a

multi-aperture telescope). To this purpose, the set of telescopes (sub-apertures) must observe simultaneously the object while maintaining constant, within a fraction of wavelengths, the phase of the various wavefronts, which are combined together (so to fulfill the coherence and co-phasing conditions, and to operate consequently like an interferometer). The utilization of an optical system constituted by a set of smaller apertures equivalent for resolution to a single monolithic mirror telescope brings considerably advantages in terms of mass saving and reduction of the storage volume.

The scope of this paper is to present concept for a high resolution imaging system, based on the utilization of an optical interferometer and the aperture synthesis technique, for future military surveillance missions from GEO.

## High resolution imagery from GEO

The maximum theoretical angular resolution provided by an aberration-free optical system characterised by an aperture of diameter  $D$  observing an object at a distance  $R \gg D$  at the wavelength  $\lambda_0$  is given by  $\lambda_0/D$ . This means that an object with a size  $l = R \cdot \lambda_0/D$ , belonging to a given scene emitting radiation at the wavelength  $\lambda_0$ , is still distinguishable inside the scene itself, when the latter is observed from a distance  $R$  with a telescope of aperture  $D$  (in the assumption that the collected radiation is sufficient to get a  $SNR \gg 1$ ).

Figure 1 shows the maximum theoretical on-ground spatial resolution achievable at the sub-satellite point for observations from LEO (800 km = Envisat-1 mean orbit altitude) and from GEO, as function of the telescope aperture diameter and for different observation wavelengths, belonging to visible (VIS: central wavelength  $\lambda_0 = 0.63 \mu\text{m}$ ), near infrared (NIR:  $\lambda_0 = 0.86 \mu\text{m}$ ), mid infrared (MIR:  $\lambda_0 = 3.7 \mu\text{m}$ ), thermal infrared (TIR:  $\lambda_0 = 10 \mu\text{m}$ ) bands.

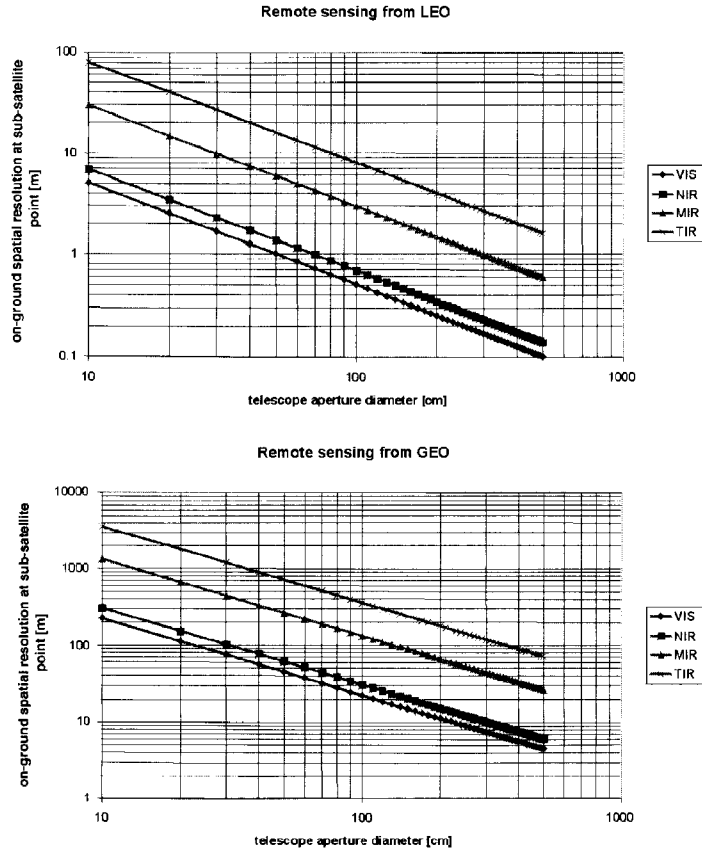


Figure 1 – Maximum theoretical on ground spatial resolution versus telescope aperture diameter for different observation wavelength. VIS = visible (central wavelength  $\lambda_0 = 0.63 \mu\text{m}$ ), NIR = near infrared ( $\lambda_0 = 0.86 \mu\text{m}$ ), MIR = mid infrared ( $\lambda_0 = 3.7 \mu\text{m}$ ), TIR = thermal infrared ( $\lambda_0 = 10 \mu\text{m}$ ).

The photon flux  $N$  collected by an optical system with aperture diameter  $D$  from a portion of Earth surface with area  $A_s$ , lying at the sub-satellite point, behaving like a lambertian sources characterized by a radiance  $L$ , and observed from a distance  $R$  along the surface normal (with  $R \gg$  surface portion size), can be approximated by the expression:

$$N = \frac{L A_s \pi D^2}{4 R^2}$$

where  $L$  is expressed in photons/ $\text{m}^2/\text{s}/\text{sr}$ .

By considering the value of the Earth radiance per unit wavelength measured by the ERS2 GOME instrument ( $\sim 2 \cdot 10^{13}$  photons/ $\text{cm}^2/\text{s}/\text{sr}/\text{nm}$  around  $\lambda_0 = 0.63 \mu\text{m}$ ) the collected photon flux in a 1-nm band from a telescope of aperture  $D$  in LEO

(800 km altitude) and GEO has been computed for different areas of the observed scene.

The results are reported in the plots of Figure 2.

From these computations it turns out that even if a relatively small 1-m aperture is sufficient to collect a good photon flux ( $\sim 10^4$  photons/s) from a  $10 \text{ m}^2$  portion of the Earth surface (in a  $\Delta\lambda = 1\text{-nm}$  band around  $\lambda_0 = 0.63 \mu\text{m}$ ), an aperture of 2.25 m is required to resolve that portion of the Earth surface from GEO at the same wavelength. This discrepancy becomes more evident moving towards the infrared region of the spectrum, since the spatial resolution for a given telescope aperture decreases as the wavelength increases (an aperture  $D = 2.25 \text{ m}$  provides a resolution of  $\sim 14 \text{ m}$  at  $\lambda_0 = 0.86 \mu\text{m}$ ,  $\sim 60 \text{ m}$  at  $\lambda_0 = 3.7 \mu\text{m}$ ,  $\sim 160 \text{ m}$  at  $\lambda_0 = 10 \mu\text{m}$ ).

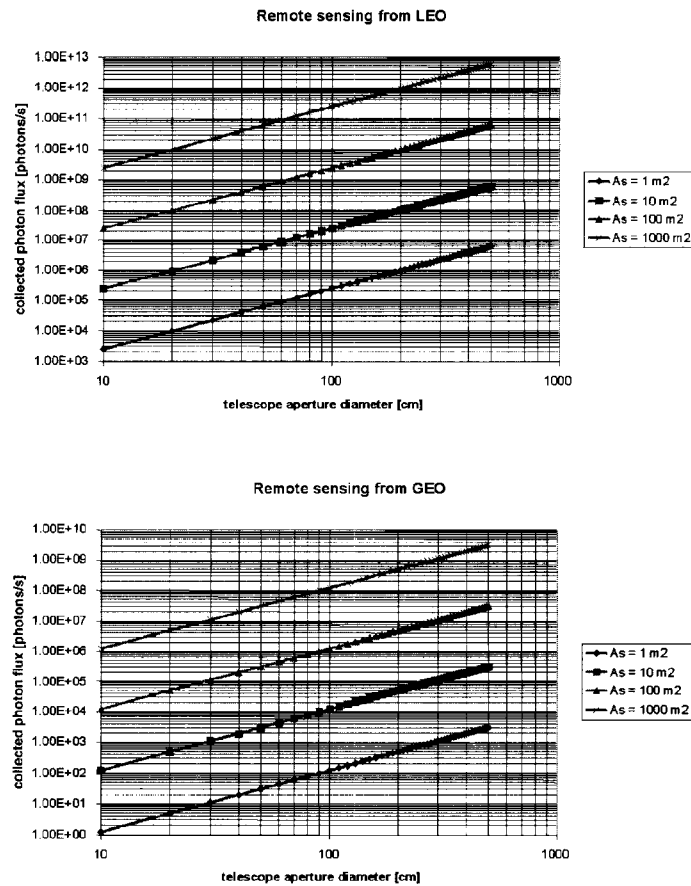


Figure 2 – Collected photon flux in a 1-nm band around  $\lambda_0 = 0.63 \mu\text{m}$  versus telescope aperture diameter, for different areas of the observed Earth surface portion (located at the sub-satellite point and observed along the surface normal).

### The optical aperture synthesis concept

With a monolithic-mirror telescope the resolution increase associated to a large aperture is paid in terms of instrument mass and storage volume. Even using the current techniques for the construction of ultra-lightweight mirrors, the mass of a 2.25 m diameter optic would be about 500 kg (see Figure 3 and ref. [1]). By comparison, the mass of the 2.48 m primary mirror of the Hubble Space Telescope is 773 kg.

A large primary mirror implies, in addition, the need of the availability of a large volume under the launcher fairing for the accommodation of the instrument.

A solution to the problems related to the large aperture, in the cases when the issue is the high

resolution and not the light collection, is represented by the synthetic aperture technique. This technique consists in the reconstruction of the original image of an object starting from that formed on the common focal plane of a set of telescopes (or a multi-aperture telescope) observing simultaneously the object while maintaining the Optical Path Differences (OPDs) between each interferometric arms much less than the so called coherence length  $l_c = \Delta\lambda/\lambda_0^2$  (to generate a fringe pattern) and the residual OPDs much less than a fraction of wavelength  $\lambda_0$  (to freeze the generated fringe pattern). That is, a multi-aperture telescope (or interferometer) can correctly work only if its telescopes are coherenced and co-phased.

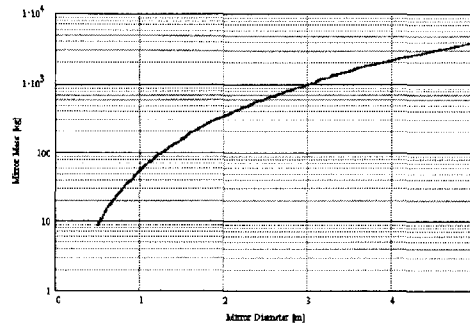


Figure 3 – Mass versus diameter relationship for ultra-lightweight mirrors (from ref. [1])

Neglecting the noise introduced by the detector, the image  $I$  of an object on the focal plane of a single-mirror telescope is given by the convolution of the “geometrical” image  $O$  of the observed scene with the Point Spread Function (PSF)  $H$  of the instrument, defined as the Fourier transform of the aperture function of the instrument:

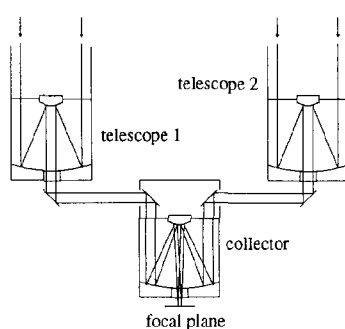
$$I = H \star O$$

This relationship holds also for the image taken by a set of telescopes correctly coherenced and co-phased. In this case the image  $I$  directly produced by the interferometer can appear even very dissimilar from the observed scene  $O$ . The latter, however, can be reconstructed through the inverse of the operator  $H$ , which exists if the Modulation Transfer Function (MTF), defined as the modulus of the Fourier transform of the PSF never drops to zero in the domain of spatial frequencies in which it is defined [2]. In this case, the reconstructed image turns out to be equal, in terms of spatial resolution, to that formed by a single-mirror

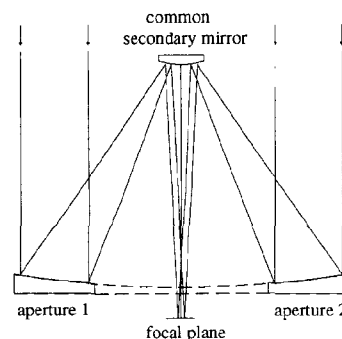
telescope with an aperture containing the set of apertures forming the interferometer.

Thus, it is possible to obtain by aperture synthesis an high spatial resolution by using in place of a large, single-mirror telescope a set of small-aperture telescopes (or a multi-aperture telescope) operating like an interferometer, provided that the total collecting areas of the smaller apertures is sufficient to guarantee a sufficient SNR on the detectors.

Two types of optical interferometer exist (see Figure 4): Michelson type interferometer, constituted by a set of single-mirror independent telescopes, and Fizeau type interferometer, constituted by a set of mirrors obtained as parts of a virtual large monolithic mirror. In the cases in which the interferometer must maintain a relatively large field of view (FOV), and the overall size of the instrument is limited to few meters, the Fizeau configuration is the solution to be preferred.



Michelson type interferometer



Fizeau type interferometer

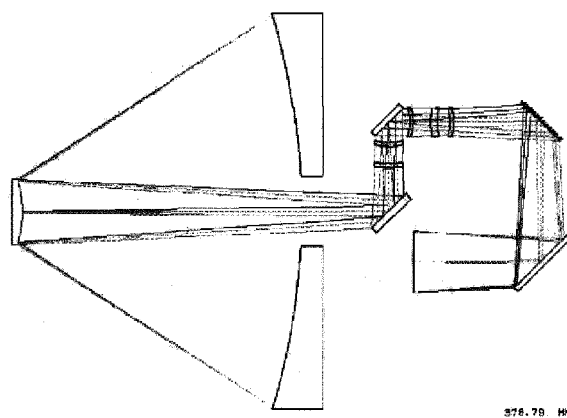
Figure 4 – Scheme of a two-mirror interferometer in Michelson and Fizeau configuration

An example of Fizeau interferometer fulfilling the  $MTF \neq 0$  criterion, has been built starting from a monolithic telescope with 2.25 m aperture designed according to the following criteria:

- diffraction-limited optical system at  $\lambda_0 = 0.63 \mu\text{m}$  over the instrument FOV;
- $FOV = 0.25^\circ \times 0.25^\circ$  (corresponding to  $\sim 150 \times 150 \text{ km}$  at the sub-satellite point from GEO);
- effective focal length = 81 m (so that a  $10 \times 10 \text{ m}$  object has a size on the focal plane =  $22.5 \times 22.5 \mu\text{m}$ )

The configuration of this telescope is shown in Figure 5. It is a two-mirror telescope with a 5-lens camera after the secondary mirror for the correction of the residual aberrations to achieve the diffraction limit condition over the  $0.25^\circ \times 0.25^\circ$  FOV at  $\lambda_0 = 0.63 \mu\text{m}$ , and a focal length of 81 m in a compact configuration.

Such a telescope can be adapted to feed several focal-plane instruments (like imagers, radiometers, spectrometers) operating in different spectral bands by replacing the camera by a set of dichroic beamsplitters for routing the light beam towards the payloads. In this case each instrument shall be equipped by its own optical system (including lenses, mirrors, prisms, gratings, polarisers,...) for matching the light beam to the features and functions of its detector. The same optical system can be designed to include the function of selecting a particular portion of the overall FOV to be observed by the detector from time to time and to change the width of the FOV seen by the detector (zoom function).



In Figure 6 the Fizeau interferometer obtained from the 2.25 m aperture monolithic telescope is shown. The large primary mirror has been replaced by a set of 4 smaller mirrors (0.7 m diameter each). Their size and relative position has been selected so to obtain a “compact” interferometer configuration, namely with  $MTF \neq 0$  over all the spatial frequencies sampled by the interferometer (the smallest of which,  $\lambda_0/D$ , corresponds to the resolution of the equivalent monolithic telescope, from which the interferometer has been obtained) and “non redundant”, namely without repetitions (in modulus and direction) among all the possible baselines joining the centers of the various mirrors (so to reduce at minimum the number of mirrors utilised).

In Figure 7 the normalized PSF and MTF of the interferometer are shown. Note that the MTF never drop to zero in the domain of spatial frequencies in which it is defined. This implies that the original scene  $O$  observed by means of this interferometer can be reconstructed through the inverse of the operator  $H$ , and the image so obtained has the same resolution as if it was taken by a 2.25 m monolithic telescope.

The set of 4 primary mirrors of the Fizeau interferometer has a total collecting area of  $1.54 \text{ m}^2$  (equivalent to that a single 1.4 m diameter mirror) and a total mass of about 82 kg (estimated with the relationship of Figure 4), about 6 times smaller than that of the single 2.25 m mirror. This dramatic mass saving, together with the possibility of folding the four mirrors in a compact launch configuration allows to accommodate a large optical system on a relatively small spacecraft.

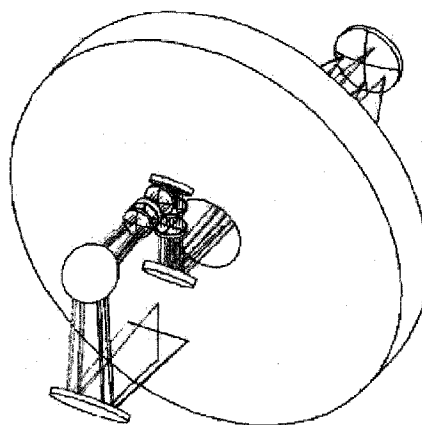


Figure 5 – The telescope with the 2.25 m monolithic primary mirror, from which the Fizeau interferometer has been obtained. After the secondary mirror the light is passed through 5-lens camera and reflected by 4 folding mirrors before the focal plane (the first folding mirror can be rotated so that the following optical system remains parallel to the plane of the primary mirror).

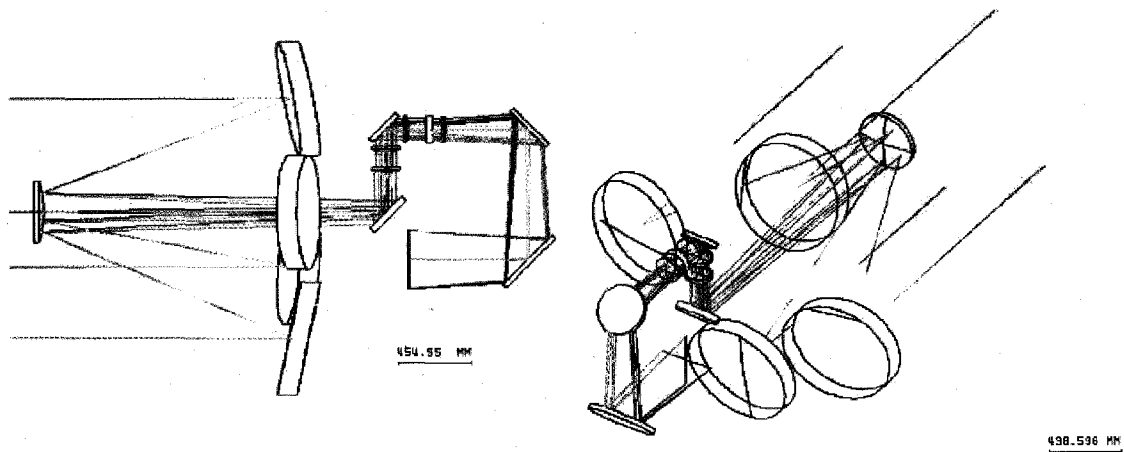


Figure 6 – Four-mirror Fizeau interferometer obtained from the 2.25 m monolithic telescope. The optics after the secondary mirror can be designed to distribute the light to various instruments.

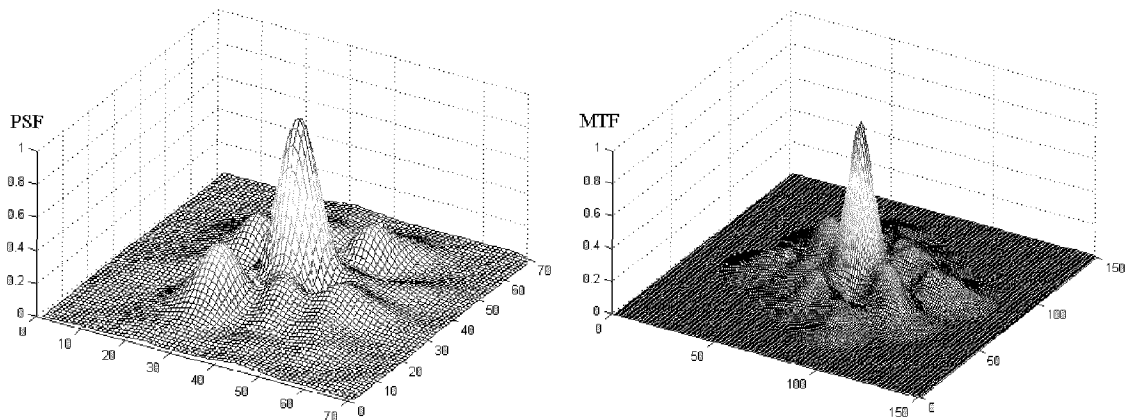


Figure 7 - Normalized PSF (left) and MTF (right) of the 4-mirror Fizeau interferometer

### Simulation results

Some first examples of the spatial resolution achievable from GEO using an instrument with 2.25 m aperture (real or synthesized) have been produced starting from two high resolution images taken from space (see Figure 8). The first one contains a  $\sim 3.5 \times 2.6$  km portion of the Santorini island taken from the IKONOS satellite (altitude  $\approx 780$  km) with a resolution of 4 meters (ref. <http://www.spaceimaging.com/level2/level2gallery.htm>). It has been used to simulate an image of the same scene as taken from GEO by the

2.25 m telescope in visible and near infrared bands ( $\lambda_0 = 0.63 \mu\text{m} \pm 0.1 \mu\text{m}$ ,  $\lambda_0 = 0.86 \mu\text{m} \pm 0.1 \mu\text{m}$ ), which provides an higher resolution. The second one contains a  $\sim 20 \times 20$  km scene of a volcanic eruption taken from the Space Shuttle (altitude  $\approx 220$  km), with a resolution of about 30 m (ref. <http://earth.jsc.nasa.gov/>). It has been used to simulate an image of the same scene as taken from GEO by the 2.25 m telescope in mid and thermal infrared bands ( $\lambda_0 = 3.7 \mu\text{m} \pm 0.1 \mu\text{m}$ ,  $\lambda_0 = 10 \mu\text{m} \pm 1 \mu\text{m}$ ), which provides a lower resolution.

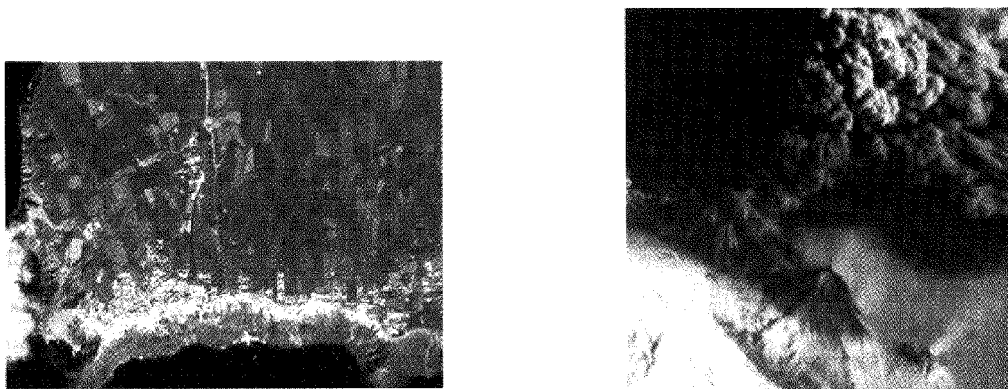


Figure 8 – High-resolution images of the Santorini island (left) and of the eruption of the Klyuchevskaya Volcano (right) taken from LEO, and used to simulate the observation of ground scenes by a GEO telescope.

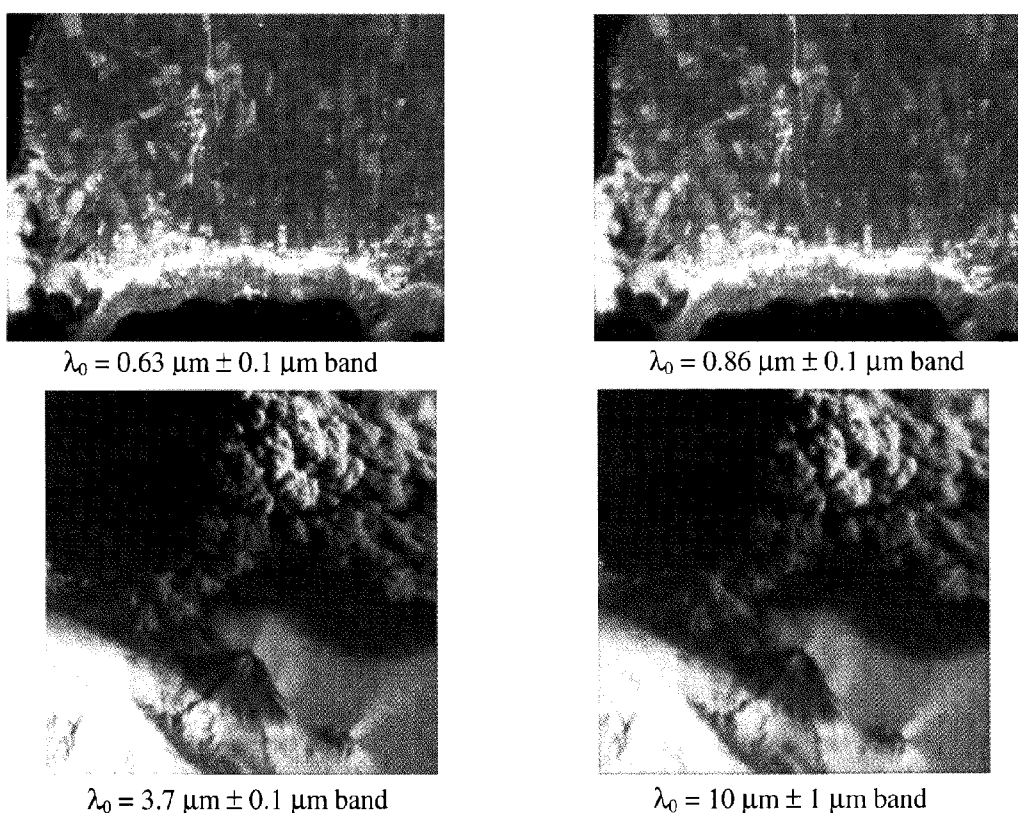


Figure 9 – Images of the Santorini island (up) and of the eruption of the Klyuchevskaya Volcano (down) as taken from GEO by a 2.25 telescope in different spectral bands (representative in terms of spatial resolution only).

These images have been convoluted with the PSF of the 2.25 m designed telescope (which includes also the residual optical aberrations) computed for the different spectral bands, and reported to the same scale of the geometrical size of the scene on the focal plane of the instrument when the latter is in GEO. The result of this operation is

representative, in terms of spatial resolution<sup>1</sup>, of the image of the scene as seen by instrument from GEO, which is the same obtainable from the interferometer shown in Figure 6, if the latter is correctly coherenced and co-phased and no errors are introduced in the scene reconstructed through the inverse of the PSF operator.

<sup>1</sup> The original images are taken in visible light. Therefore the simulated images so obtained can be considered fully representative of the scene seen by the GEO telescope only in the  $\lambda_0 = 0.63 \mu\text{m} \pm 0.1 \mu\text{m}$  band. In fact, no radiance

map relative to the emission in the infrared wavelengths has been applied to the scene for the simulation of the images in the NIR, MIR, TIR bands. The latter images, however are representative in terms of spatial resolution.



The resulting images are shown in Figure 9. The excellent image quality (in terms of spatial resolution) still achievable from GEO with a 2-m class telescope is apparent.

### Implementation and technology to be developed

The main technical problem related to the operation of such an instrument is related to its coherencing and co-phasing, i.e. the equalisation of the optical path length (OPL) of the light from the interferometer apertures to the focal plane equal within a small fraction of the coherence length ( $OPD_{ij} = |OPL_i - OPL_j| \ll \lambda_0^2/\Delta\lambda$ ;  $\lambda_0$ ,  $\Delta\lambda$  = central wavelength and width of the observation spectral band) and its stabilisation within a small fraction of  $\lambda_0$  ( $\Delta OPD_{ij} \ll \lambda_0$ ) during the image acquisition and over the whole FOV. For instance, for an observation in the visible band, with  $\lambda_0 = 630$  nm and  $\Delta\lambda = \pm 100$  nm, and considering a factor 100 for the fulfilment of the above inequalities:  $|OPL_i - OPL_j| = \lambda_0^2/(\Delta\lambda \cdot 100) \approx 20$  nm and  $\Delta OPD_{ij} = \lambda_0/100 \approx 6$  nm.

The information for the equalisation of the OPLs within the coherence length can be achieved by analyzing the image of a point-like source on the instrument focal plane, with the same technique defined for the coherencing of the mirror segments

of the Next Generation Space Telescope or of the ground optical interferometers, like the VLTI. For this operation the instrument can be temporarily pointed towards a bright star (since the angular size of the full Earth seen from GEO is  $17.4^\circ$ , a relatively small slew manoeuvre is required to move the interferometer boresight axis from the Earth disk to the starry sky and vice versa).

For instance, with reference to the 2.25 Fizeau interferometer design described in section "High Resolution Imaging from the Geostationary Orbit", a star image produced by the instrument once the coherence condition has been achieved shall look like that shown in Figure 10.

The OPLs equalisation can be performed by moving the primary mirrors in three DOF's (one piston along the mirror axis and two tilts of the mirror plane) by means of 3-DOFs tip-tilt mechanisms, like, for instance that shown in the Figure 11. Each mechanisms is composed by three linear actuators, placed at  $120^\circ$  around the mirror. Each actuator is made in two stages: a long-range coarse stage, constituted by a stepper motor (covering a millimeter-level stroke with micrometer resolution) and a short-range fine stage, constituted by a piezoelectric translator (covering a micrometer-level stroke with nanometer resolution).

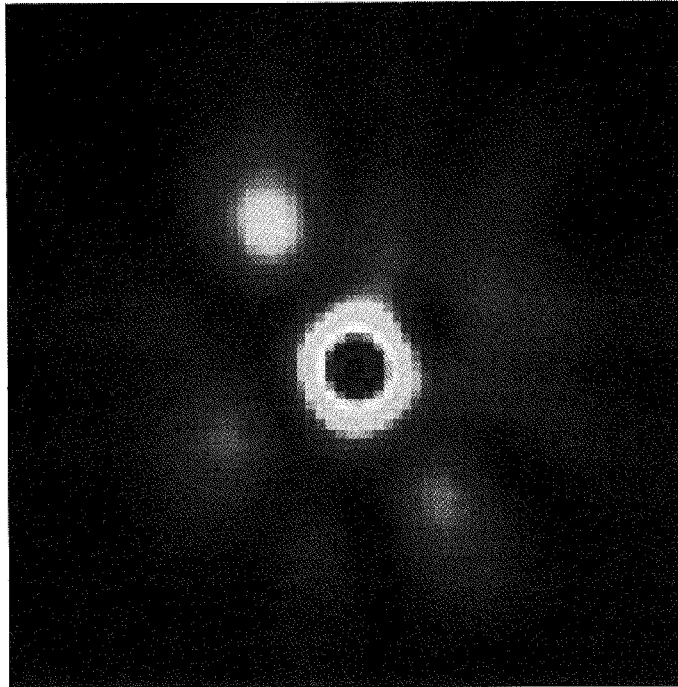


Figure 10 – Image of a pointlike source produced by the 2.25 m Fizeau interferometer after the equalisation of all the optical paths lengths of the light from the apertures to the focal plane.

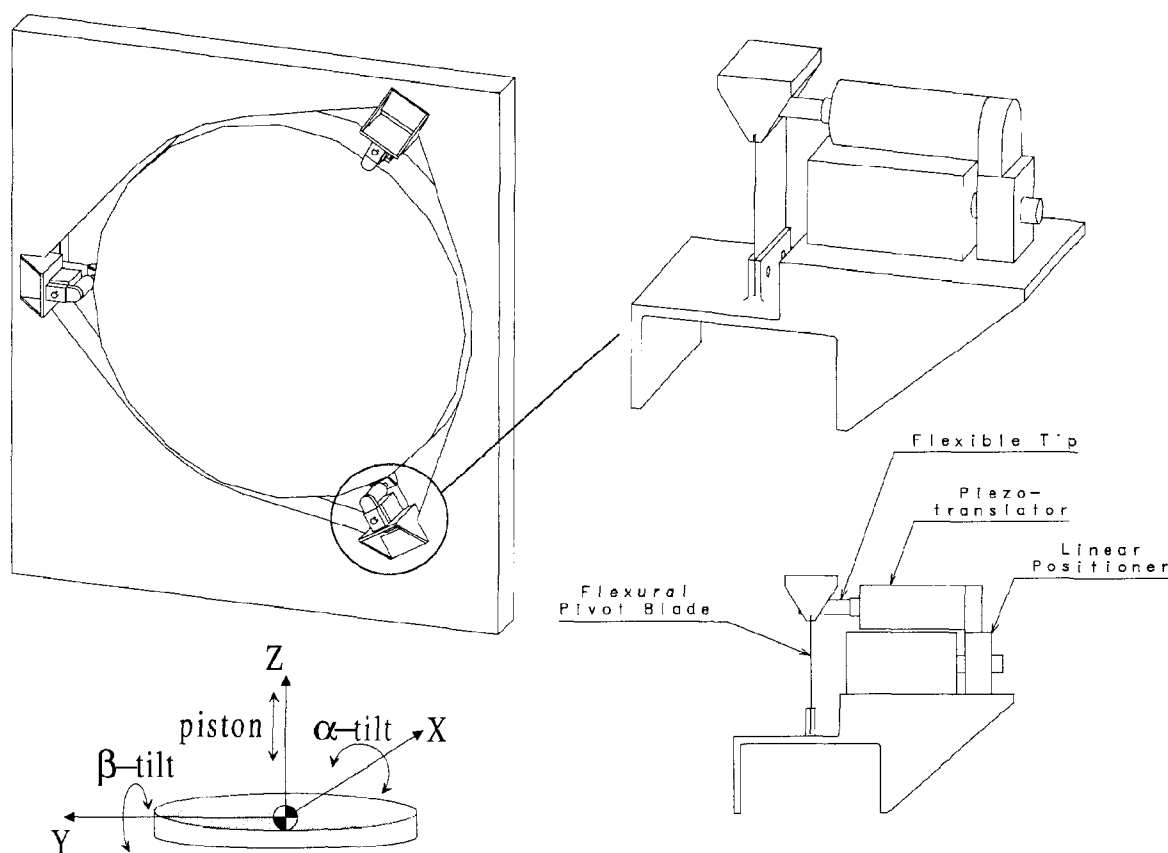


Figure 11 – Example of tip-tilt mechanism for the control of the interferometer primary mirrors

Once the coherence condition has been achieved, the co-phasing condition can be maintained without reference to external sources, by measuring by means of laser interferometers the relative position between optical reference markers suitably placed on the primary and the secondary mirrors (see Figure 12) and commanding the tip-tilt mechanisms so that to maintain stable the measured distances. In fact, the optical path from the secondary mirror to the focal plane is mostly common to light entering through all the interferometer apertures, therefore significant optical path difference can be originated only between the primary mirrors and the secondary mirror.

While the interferometer co-phasing is maintained in this way, the instrument can be re-pointed towards the Earth to perform the planned remote-sensing observations.

The possibility of achieving the coherence condition by means of tip-tilt mechanisms and to maintain the co-phasing by means of such an optics active control system (based on laser metrology and tip-tilt mechanisms) has been demonstrated by Alenia Aerospazio, by means of

analyses and simulations performed by suitable software tools, within the ESA TRP contract “Active Pointing of Large Telescopes and Attitude Measurement Transfer Systems”(APLT & AMTS) for a two-aperture Fizeau interferometer designed for the future astrometric mission GAIA (ref. [3]). Within the same study, a laboratory prototype of the optics active control system has been implemented and tested on a special test-bed (named Control Optics Structure Interaction - COSI – Test-bed). The metrology system consists of three Fabry-Perot interferometers fed by a Nd:YAG laser source at 1064 nm, frequency stabilised against a reference optical cavity using the Pound-Drever technique. The test purpose was the verification of the system performance in the stabilisation of the distances between three pairs of optical elements placed on two  $\varnothing = 57$  cm plates (simulating two GAIA mirrors) at a 0.5 m relative distance (see Figure 4). The achieved distance stabilisation was better than **3 pm**, under the seismic and acoustic vibrations coming from the laboratory environment and the application of sinusoidal disturbances with 1  $\mu$ m amplitude to one of the plates (ref. [4]).

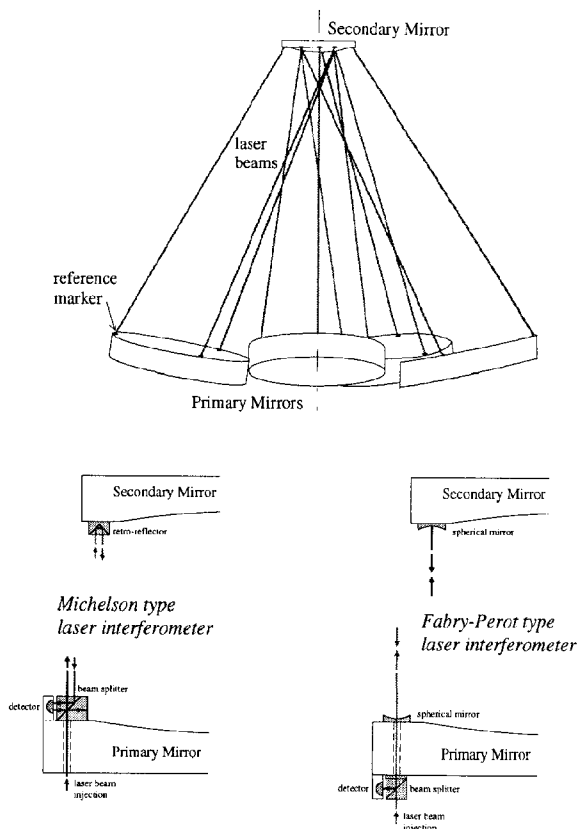


Figure 12 – Example of laser metrology system for the distance measurement between reference optical markers placed on the primary and secondary mirrors, to be used for the interferometer co-phasing. The laser interferometer utilised can be of two types: Michelson (concept shown on the left), or Fabry-Perot (concept shown on the right).

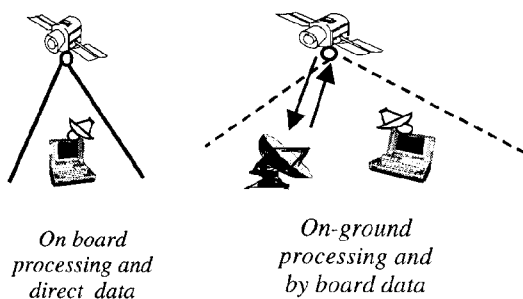


Figure 13 – Data processing and dissemination concepts

## Conclusions

From the military and risk management applications point of view the availability of a continuous observation capability and a real time data delivery constitute an invaluable asset. Despite the one meter spatial resolution needs 25 meters diameter optic, for a five meters resolution only five meters telescope would be necessary. Then effective change detection can be implemented to support EW, treaty verifications, law enforcement, fire detection, disaster monitoring, etc. Five meter diameter value fits with the Ariane V firing dimension therefore the system can be launched avoiding complex folding architectures. The data processing and dissemination take benefit from the specificity of Geo orbit that permitting the direct transmission of the data to ground in a raw format or after the on board processing (see fig. 13). Alenia Spazio is studying the system concepts and the technologies to implement the such GEO system which could be deployed in 7-10 years from now.

## References

- [1] Valente T. M. – *Scaling laws for light-weight optics* – Cryogenic Optical Systems and Instruments IV, SPIE Vol. 1340, 1990
- [2] J. W. Goodman – *Introduction to Fourier Optics* – McGraw-Hill, New York, 1968
- [3] S. Cesare, C. Philippe – *Developments of enabling technologies for the GAIA mission* – Proceedings of the 49 International Astronautical Congress, IAF-98-Q.1.06, September 1998
- [4] M. Bisi et al. – *Investigation of enabling interferometric technologies for the GAIA astrometric mission* – Proceedings of SPIE "Interferometry '99", Vol 3744, September 1999.